

2. Research methodology

Cobalt-chromium alloy with the chemical composition determined by X-ray spectroscopy (XRS 300 spectrometer, Siemens) (TABLE 1) was used as the study material. Rods, 45mm long and 2.5 mm in diameter, were cast from the alloy and sandblasted with Al_2O_3 with the average grain size of 50 μm . X-ray analysis of each rod was performed (Baltosot GFD165 HAND-X, Balteau), in order to control the cast quality. Any casting defects were assessed based on the PN-EN 12681 standard and those elements were discarded, in which porosities and blowholes were found.

TABLE 1
Chemical composition of the alloy used in the experiment

Chemical composition [% w/w]				
Co	Cr	Mo	Si	Mn
the remainder	31.56	5.53	0.64	0.72

Finally, 30 rods with no casting defects were selected for the tests. The layer of oxides was removed from the samples in an ultrasonic washer and the samples were divided into 3 groups, 10 rods in each. Group 1 was the control group, groups 2 and 3 were study groups, in which the samples were welded or soldered. Samples from the study groups were fixed in a special holder, cut in half with a diamond disc with the diameter of 0.4 mm, in the plane perpendicular to the long axis.

Samples in group 2 were joined with a propane-butane gas burner. The cut metal was put together in a way which preserves the standard space required in traditional soldering, using a spacing washer with the diameter of 0.4 mm, which was then removed after the samples were fixed in the holder. Solder intended for joining cobalt-chromium-based alloys (Denti-Lot, Elephant Dental B.V. Hoorn) was used for soldering. Samples after soldering were cooled down and sandblasted with Al_2O_3 with the grain diameter of approx. 50 μm .

Samples in group 3 were welded with a laser beam. Laser butt welding, in the shape of the letter I, was performed in the presence of solder in the form of wire with the diameter of 0.25 mm (Ankatit, Anka Guss GmbH), with the two separated parts in a close contact in the holder. A laser (Nd Yag Laser Titec model XXS, Orotig) with the wavelength of 1064 nm and the parameters $E = 25 \text{ J}$, $t = 0.5\text{--}8 \text{ ms}$, $P = 30 \text{ W}$, was used in the test, with each next laser beam focus overlapping the previous one, at least in 75%. The size of the laser beam was selected after preliminary tests and they were: power 1.8 W, frequency 3 Hz and the impulse duration 2.5ms.

After the processes of welding and soldering were completed, the rods were again examined by X-ray defectoscopy in order to eliminate the samples with disqualifying welding defects. The quality of the joints was assessed based on the PN – EN-ISO 6520:2002 and PN – EN-ISO 5817:2007 standards. Subsequently, all the samples were polished by the standard procedures.

The samples were used in testing the joint for tensile strength, impact strength and fractographic examinations.

In order to make the tests repeatable, all the samples were shaped as recommended by the standards. The joints were turned on a lathe to create a narrowing required in tensile strength tests. This reduced the crosswise dimension from 2.5 mm to 2 mm.

In order to analyse the joint strength, a tensile strength test was carried out with the use of a universal strength tester (Zwick–Roel Z100; Zwick GmbH & Co, Ulm), in accordance with the PN-80/H 04310 standard. The elongation rate of 0.5 mm/min was adopted in the test. The sample strength was recorded by a computer coupled with the tensile strength tester. An extensometer was used to measure the changes of linear dimensions (Fig. 1).

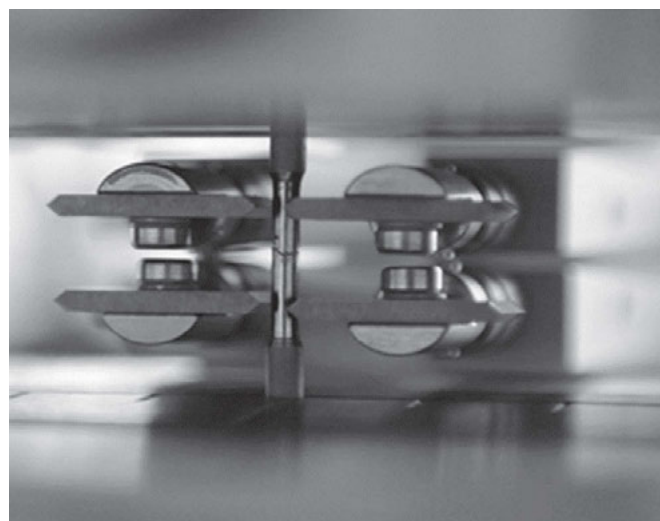


Fig.1. A sample in a tensile strength tester with extensometer arms installed

Elements of prosthetic structures are often subjected to large dynamic loads during their use. Although an impact amplitude does not exceed the largest acceptable load, an element may be destroyed. Hence, it was regarded as justified to perform an impact strength test.

The impact strength test was carried out in accordance with the PN-68/C-89028 standard using a Dynstat apparatus (Werkstoffprüfmaschinen Leipzig), intended for testing finished and semi-finished products whose dimensions prevent the tests being performed by any other method (Charpy or Izod), which was the case with the samples in question due to their small size. Rods with a notch made at the joint were used in the tests. Impact strength of a sample was determined as work used to break a sample dynamically, referred to the cross-section of 1 mm².

Fractographic examinations were used in order to analyse the fractures. The method helps to identify the nature of material cracking, the material zones with the most critical strains, which is a source of information about the cracking mechanism. The examinations were performed under a scanning electron microscope (Hitachi S-3000N). Fractures of samples after the tensile strength test were analysed at the magnification of several dozen to several thousand times.

TABLE 2

Results of the tensile strength test and the maximum elongation of all the samples under study depending on the joining technique. R - the maximum stress applied to a sample in the tensile strength test [MPa]. A - relative elongation, %. The average values are provided under the table.

No.	Group 1. Solid samples		Group 2. Soldered (gas-welded) samples		Group 3. Laser-welded samples	
	R {lo m} [Mpa]	A {lo gt} [%]	R {lo m} [Mpa]	A {lo gt} [%]	R {lo m} [Mpa]	A {lo gt} [%]
1	754	2.8	348	0.1	624	1.7
2	538	3.0	225	0.1	513	5.5
3	491	1.2	499	0.5	625	1.2
4	424	0.5	233	0.2	580	2.3
5	585	1.0	426	0.4	615	4.1
6	469	3.2	691	4.8	480	3.2
7	579	6.5	530	1.6	542	3.0
8	707	2.8				
9	618	5.0				
Mean	573.9	2.9	421.7	1.1	568.4	3.0
St dev	108,3	1,9	168,3	1,7	58,0	1,7

3. Results and discussion

3.1. Tensile strength

The strength tests conducted in accordance with the standard procedures of tensile strength tests produced results shown in TABLE 2. The strength of the joints ranged from 424 MPa to 754 MPa for the solid material, from 225 to 691 MPa for samples joined by traditional soldering and from 480 to 625 MPa for the material joined with a laser beam.

The results were analysed statistically with the use of *Kruskal-Wallis* and *Wilcoxon* test. The analysed quantities included the maximum stress applied to a sample during the tensile strength test, R [MPa] and the relative elongation A [%] and the aim of the analysis was to examine the statistical relationship between the tensile strength of samples joined by various techniques (with a gas burner and laser-welded). The first step of the tensile strength analysis of the joints obtained in the experiment involved making preliminary calculations for the *Kruskal-Wallis* test, which verified a hypothesis of identical distributions of the R {lo m} variable in all the three material groups. The results of the *Kruskal-Wallis* test performed at the level of significance of $\alpha=0,05$ provided grounds for rejecting the hypothesis of identical distributions of the R {lo m} variable in all the groups, which means that a comparison of collective results reveals statistical differences in the results of tensile strength tests for all the examined groups.

Similar conclusions can be drawn by analysing the maximum elongation of a metal sample. The results of the *Kruskal-Wallis* test performed at the level of significance of $\alpha=0,05$ provided grounds for rejecting the hypothesis of identical distributions of the A {lo gt} variable in all the groups of materials. The hypothesis is also rejected at the level of $\alpha = 0.01$, for which $\chi^2_{3,1-\alpha} = 11.345$. Therefore, there is a significant difference of the maximum elongation observed in all the samples under study.

The results of the *Wilcoxon* test have shown that there

are no grounds at the level of significance of $\alpha = 0.05$ for rejecting the hypothesis that the distributions of the R {lo m} variable in group 1 (solid samples) and in group 2 (soldered samples) do not differ significantly. Similar results were obtained by analysing the distributions of the R {lo m} variable for groups 1-3 (solid - welded), groups 2-3 (soldered - welded). The differences are random in character. On the other hand, the results of the *Wilcoxon* test have shown that there are significant differences at the level of significance of $\alpha = 0.05$ between the distributions of the A {lo gt} variable in group 2 (soldered samples) and in group 3 (welded samples).

An analysis of the maximum elongation observed in the strength tests shows that there are significant differences between samples joined by the traditional soldering technique and samples in the other study groups. This means that the elongation of samples joined by gas welding is the smallest and ranges from 0.1% to 4.8%, whereas the values for the solid samples range from 0.5% to 6.5% and for the welded ones - from 1.2% to 5.5%. Differences were also observed between the results for the other groups, but they are not as significant as those for the gas-welded samples.

The results of the experiment show that deformations and breakage of the samples took place in the joint area, but that the force required for breaking a joint had to be greater - for the material joined with a laser beam - by about 150 MPa compared to the group in which samples were gas-welded. Moreover, the experiments showed that the maximum elongation is also observed in laser-welded samples. The elongation did not exceed 1% in over 85% of the soldered samples with the average for the group equal to 1.1%. The average values in the other groups were: 2.9% (solid) and 3.0% (welded).

3.2. Impact strength tests

The results of the impact strength tests are shown in TABLE 3.

TABLE 3
The results of the impact strength tests of the joints

Sample number	Impact strength [J/mm ²]		
	Solid samples	Gas-welded samples	Laser-welded samples
1	40.0	13.3	28.4
2	44.4	23.1	32.0
3	35.6	20.4	36.9
4	40.9	16.9	32.0
5	40.0	19.1	30.2
Mean	40.2	18.6	31.9
Standard deviation	3.2	3.7	3.1

The results were analysed statistically with the use of *Kruskal-Wallis* and *Wilcoxon* test, by a similar procedure as in the tensile strength test. The analysis has shown that the impact strength of the gas-welded samples is much lower than that of the others. The differences are statistically significant. The smaller impact strength is probably the result of insufficient melting of the solid material in the joint area and, consequently, its worse joining. Although there are observable differences between the impact strength between the other groups of samples, they are not statistically significant. The impact strength of the laser-welded samples is similar to that of the solid material.

3.3. Fractographic analysis

Fig. 2, 4, 6 show selected images of fractures of samples after the tensile strength test, obtained under a scanning electron microscope, whereas fig. 3, 5, 7 show similar images from an optical microscope of fractures of destroyed samples.

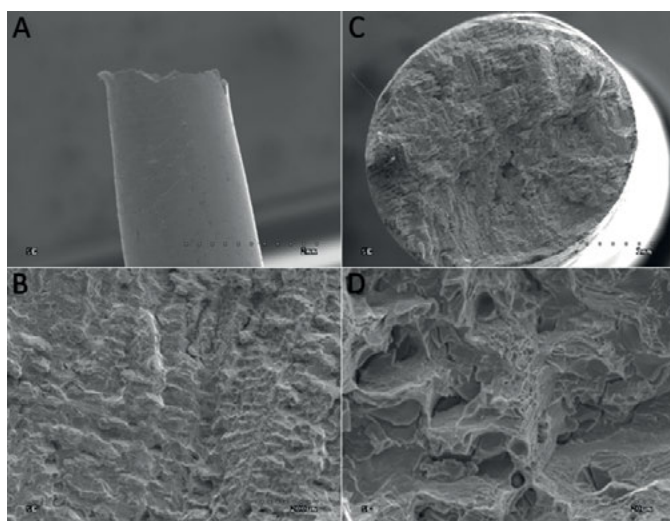


Fig. 2. Microscopic images of fractures of the solid material. A - General view of the sample, B - General view of the fracture, C - Magnified fracture in the dendrite area, D - Magnified fracture in the mixed fracture area

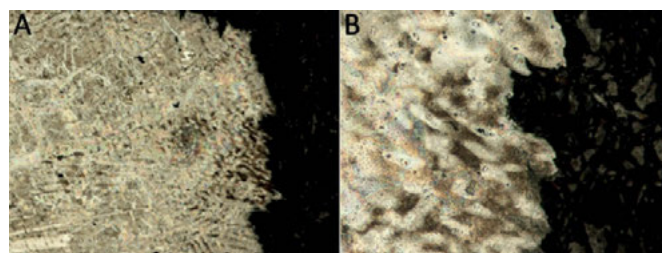


Fig. 3. Microscopic images of fractures of the solid material. A - A sample cross-section in the fracture (magn. x 50), B - Sample cross-section – magnified fragment (magn. x 200)

The fractographic examination conducted with the control group (solid material) showed that the fracture of solid material is an intercrystalline fracture between dendrites (Fig. 2b, c). The general view of the sample shows a distinct narrowing (Fig. 2a), which is indicative of a certain plastic deformation during the process of cracking. This is confirmed by the presence of some areas of ductile fracture, visible in Fig. 2d. These results are consistent with those of the tensile strength test. Overall, the nature of the fracture is mixed (plastic and brittle). Small plastic deformations in the fracture area are also visible in optical microscopic images (Fig. 3).

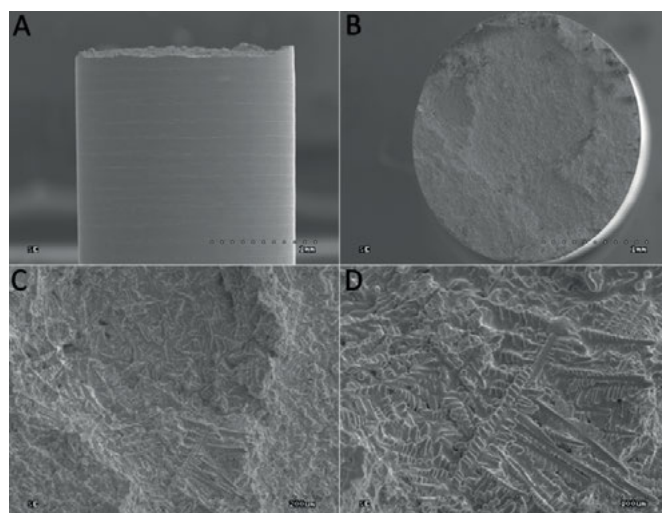


Fig. 4. Microscopic images of fractures of gas-welded samples. A - General view of the sample, B - General view of the fracture, C - The fracture area in the dendrite zone, D - Magnified fracture in the dendrite zone

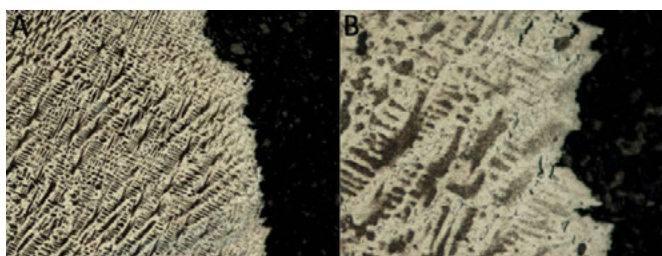


Fig. 5. Microscopic images of fractures of gas-welded samples. A - A sample cross-section in the fracture (magn. x 50), B - Sample cross-section – magnified fragment (magn. x 200)

Fractures of gas-welded (soldered) samples are similar in character to those of the solid material. The fractures in this case are also intercrystalline (Fig. 4b, c). However, the fracture

observed here is more microcrystalline, and the dendrites visible in it are distinctly smaller. This is also visible in the photograph of the fracture area, obtained under an optical microscope (Fig. 5a, b). The dendritic structure is also visibly finer than in the solid material. This could be caused by much faster cooling down in gas-welding than in the casting process. In this case, supercooling of liquid metal in the joint area is deeper than that of liquid metal during the casting process and, according to Tamman's rule of crystallisation, a structure of small grain size is obtained. In this type of welding, one should expect a more microcrystalline structure in the material part more distant from the joint. Since the area of material heated during gas-welding is much larger than during laser-welding, its temperature increase followed by cooling down is a kind of thermal treatment, which can contribute to producing smaller grains. The general view of the sample (Fig. 4a) does not reveal any distinct plastic deformation. The nature of the fracture is much more brittle (there are hardly any areas of ductile fracture).

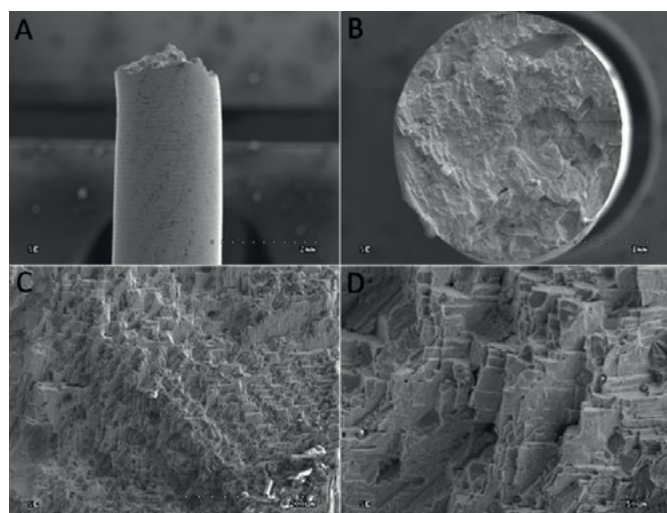


Fig. 6. Microscopic images of fractures of laser-welded samples. A - General view of the sample, B - General view of the fracture, C - The fracture area in the dendrite zone, D - Magnified fracture in the brittle fracture zone

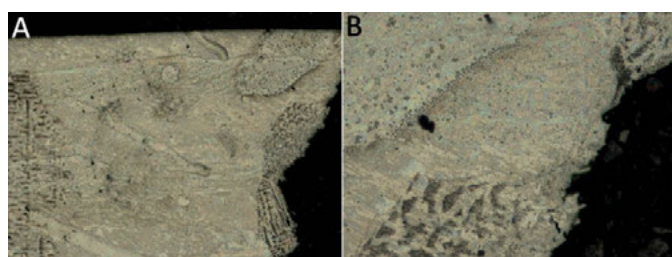


Fig. 7. Microscopic images of fractures of laser-welded samples. Sample cross-section at the fracture site A - magn. x 50, B - magn. x 200

Fractures in laser-welded samples are brittle and transcrystalline (Fig. 6b, c). No primary dendrites are visible in the photographs. However, small plastic deformations are visible (Fig. 6a), but areas of ductile fracture occur only sporadically. Interesting results have been gained from

observation under an optical microscope. The images show etched areas (a dendritic structure formed during the process of casting) and unetched areas (joint). It seems that in most cases, cracking took place on the joint border - between the joint and the solid material (Fig. 7a, b). This indicates good strength of the weld, which is at least as high as that of the solid material. The area of joint obtained by laser-welding shows an increase in the joint strength, which is confirmed by strength tests. This is an important criterion in the selection of a method of joining prosthetic structures. Images taken under an optical microscope also show defects in the form of small blowholes. Their formation is probably caused by a small width of the gap, which makes it difficult for molten metal to flow into it.

4. Conclusions

- The experiment and its analysis lead one to the following conclusions:
- Metal elements used to make prosthetic fillings, joined by the technique which uses a laser beam, have better strength properties than those achieved by gas welding.
- The strength properties of laser-welded elements are similar to those of a solid material.
- Therefore, the technique of laser joining of metal structure is a better option in repair and making of dentures than gas welding.
- Surface preparation prior to laser welding should be considered so that the laser beam can penetrate the full depth of the metal, thereby ensuring better mechanical properties.

The research was made in Medical University of Lodz and in Lodz University of Technology.

REFERENCES

- [1] N. Shigeto, T. Yanagihara, T. Hamada, E. Budtz-Jørgensen, *J Prosthet Dent* 62, 512 (1989).
- [2] A.B. Carr, R.B. Steward, *J Prosthodont* 2, 2 (1993).
- [3] E.M. De Torres, R.C. Rodrigues, G. de Mattos, R.F. Ribeiro, *J Dent* 35, 800 (2007).
- [4] A-H. Shehab, M. Pappas, D.R. Burnes, H. Douglas, P.C. Moon, *J Prosthet Dent* 93, 148 (2005).
- [5] S.F. Rosenstiel, M.F. Land, J. Fujimoto, *Współczesne protezy stałe*, Lublin 2001.
- [6] J. Brudvik, S. Lee, S.N. Croshaw, D.L. Reimers, *Int J Prosthodont* 21, 285 (2008).
- [7] T. Gordon, D.L. Smith, *Quintessence Int* 3, 63 (1972).
- [8] R. Tiozzi, R.C.S. Rodrigues, M. Chiarello de Mattos, R.F. Ribeiro, *Int J Prosthodont* 21, 121 (2008).
- [9] G.E. Goll, *J Prosthet. Dent* 66, 377 (1991).
- [10] G.A. Zarb, A. Schmitt, *J Prosthet. Dent* 64, 53 (1990).
- [11] G.P. McGivney, A.B. Carr, *Ruchome protezy częściowe w ujęciu McCrackena*, Lublin 2002.
- [12] M. Hajduga, B. Kalukin, *Nowoczesny Technik Dentystyczny* 1, 36 (2007).

